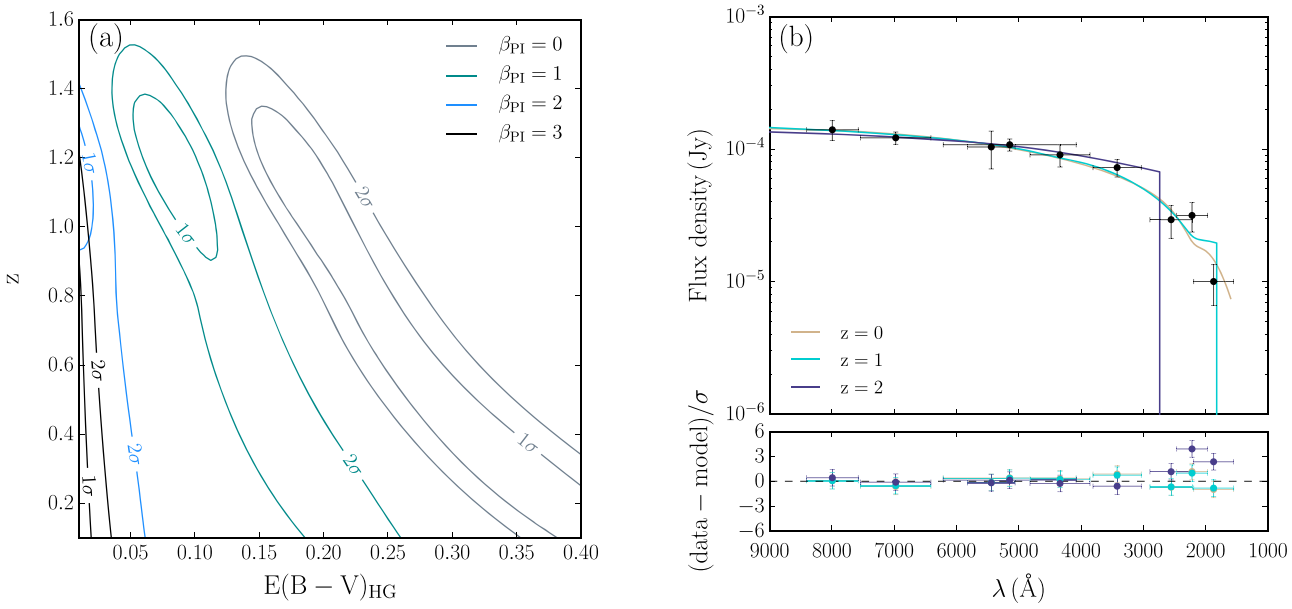

Figure 8. Estimation of the GRB 180618A redshift from the co-temporal GRB 180618A UVOT and RINGO3 data modeled with a dust-absorbed power law that includes the redshifted Lyman-limit break. (a) χ^2 distribution of the best-fitting redshifts for different values of the host galaxy extinction $E(B-V)_{HG}$ and photon index β_{PI}. The confidence level contours at the 2σ level indicate a redshift $z < 1.5$ for GRB 180618A. (b) Best-fitting models for redshifts $z = 0$, 1, 2.

Table 2
GRB 180618A Optical Photon Indexes ($\beta_{opt,PI}$) Derived from the Best-fitting Power-law Models to the RINGO3 Data

t_{mid}-T_0 (s)	t_{err} (s)	$\beta_{opt,PI}$	$\beta_{opt,PI,err}$
231	30	0.7	0.4
340	42	1.2	0.4
473	89	1.2	0.4
749	179	1.3	0.4
995	67	1.5	0.4
1212	150	1.4	0.4
1528	90	1.2	0.4
1825	208	1.8	0.5
2670	298	2.6	0.6
3288	298	4.0	0.8

Note. t_{mid} is the mean observing time, T_0 is the BAT trigger time, and t_{err} is half the length of the observing time window. Note that the model does not account for host galaxy extinction.

redshift $z < 1.5$ at the 2σ confidence level from the $E(B-V)_{HG} - \beta_{PI} - z$ parameter space (see Figure 8(a)). Note that not knowing the GRB 180618A intrinsic spectral slope does not affect the redshift constraint but adds large uncertainty in determining the host galaxy dust contribution. See also the best-fitting models for redshifts $z = 0$, 1, 2 in Figure 8(b).

Among all three candidate galaxies detected in the LBT images, G1 is the most likely host galaxy of GRB 180618A given its proximity (see Figure 3). In the G1 galaxy spectrum (see Figure 5), we detect two emission lines at $\lambda_{obs,O\,II} = 5794.8$ Å and $\lambda_{obs,O\,III} = 7784.0$ Å, corresponding to the unresolved [O II] $\lambda = 3726$–3729 Å doublet and the [O III] $\lambda = 5007$ Å line, respectively. This implies a spectroscopic redshift of $z_{G1} = 0.554 \pm 0.001$ for the G1 galaxy. This value is consistent with O'Connor et al. (2022) and Nugent et al. (2022) estimates of photometric redshifts of $z = 0.4^{+0.2}_{-0.1}$ and $z = 0.52^{+0.09}_{-0.11}$, respectively. We find that the probability of an accidental alignment (Bloom et al. 2002; Berger 2010; Fong & Berger 2013) of GRB 180618A and the G1 galaxy is low, with $p_d \approx 0.02$. Therefore, we associate the G1 redshift ($z = 0.554$) with GRB 180618A. For the G2 galaxy spectrum, we do not detect emission lines. However, there is a clear drop of the continuum flux blueward of $\lambda_{obs} \approx 6200$ Å that we identify as the $\lambda = 4000$ Å break, corresponding to a redshift of $z_{G2} \approx 0.55$. Therefore, the LBT spectroscopic analysis suggests that all three galaxies (G1, G2, and G3) are at a similar redshift.

GRB 180618A lies in the outskirts of its host, 10 kpc from the center of the galaxy (see also O'Connor et al. 2022; Fong et al. 2022). This is consistent with the large offsets found in short GRBs and in disagreement with those of long GRBs (Berger 2010; Fong & Berger 2013; Behroozi et al. 2014; Fong et al. 2022). Note that short GRBs are usually found with offsets to star-forming disk galaxies or even further away from their elliptical host (Fong & Berger 2013; Behroozi et al. 2014). Similar to the environment of GRB 180168A, Fong & Berger (2013) found that about 30%–45% of short GRBs happen where there is no optical light, i.e., negligible stellar mass. Like GRB 180618A, most short GRBs display signs of migration from their birth sites, likely due to natal kicks in binaries (Rosswog et al. 2003; Kelley et al. 2010; Fong & Berger 2013). This is consistent with short GRBs exploding in low ambient density, thus producing fainter afterglows (Berger 2010; Kann et al. 2011; Fong et al. 2015).

3.3. Duration of the Prompt Gamma-Ray Emission

We calculated the duration (T_{90}) of GRB 180618A (Lien et al. 2016; Moss et al. 2022), corresponding to the time interval in which 90% of the burst fluence is released, using the 64 ms binned and background-subtracted GRB 180618A light curves of the BAT. Using the *battblocks* tool (Scargle 1998), a *FTOOLS* released as part of *HEASoft* (Blackburn 1995), we find $T_{90} = 45 \pm 10$ s for the low-energy spectral range of the BAT (i.e., 15−100 keV), and $T_{90} = 0.26 \pm 0.14$ s at 100−350 keV. The duration of GRB 180618A at the low-

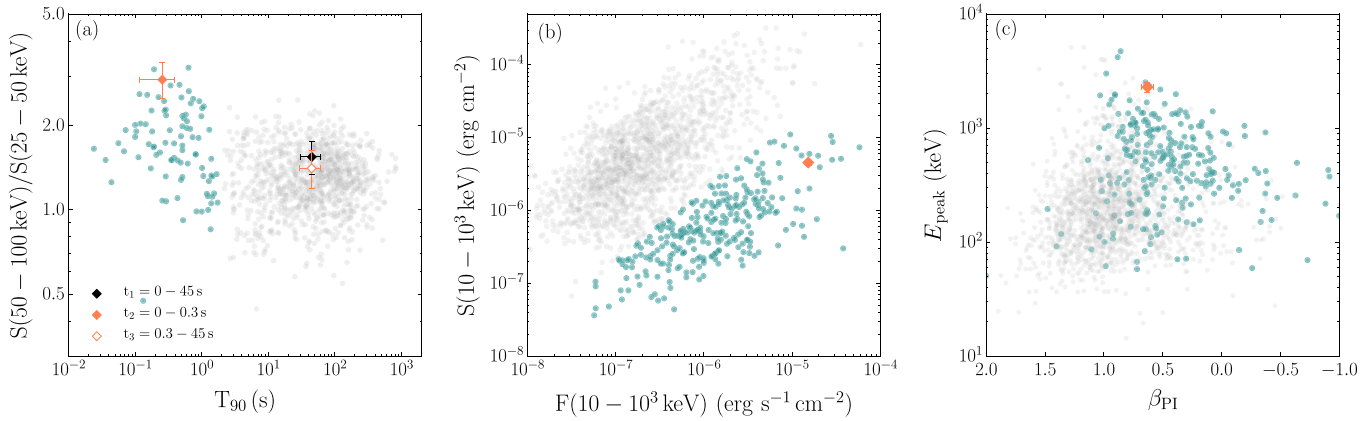

Figure 9. High-energy properties of GRB 180618A and comparison with catalog GRBs; those with duration $T_{90} > 2$ s are displayed in gray, and those with $T_{90} < 2$ s in blue (Kouveliotou et al. 1993). (a) BAT-band hardness ratio and duration of GRB 180618A (t_1), the ≈0.3 s short gamma-ray pulse (t_2), and its ≈45 s extended gamma-ray emission (t_3). The background data correspond to the short hard and long soft bimodal clustering of the BAT GRB catalog (Kouveliotou et al. 1993; Lien et al. 2016). (b) Comparison of the ≈0.3 s short GRB 180618A flux F and the fluence S (marked in orange) with the GRB sample from the GBM catalog (von Kienlin et al. 2020; Poolakkil et al. 2021). Note that the GRB 180618A flux and fluence have been recalculated to match the $10-10^3$ keV energy range of the GBM catalog. (c) Photon index β_{PI} and peak energy E_{peak} of GRB 180618A (marked in orange).

energy bands is 2 orders of magnitude higher than at high-energy bands, confirming two spectral components: a short hard GRB and extended soft gamma-ray emission below the 100 keV energy band (Hamburg et al. 2018; Sakamoto et al. 2018; Svinkin et al. 2018). We find that the 0.3 s short-duration GRB 180618A belongs to the hardness–duration cluster of short GRBs, and that it is one of the hardest to have been detected by the BAT (within the top ≈0.5%; see Figure 9-a). Note also that Sakamoto et al. (2018) found negligible spectral lag for the short-duration gamma-ray pulse of GRB 180618A —a spectral property typical of short hard GRBs.

Furthermore, GRB 180618A is a classically short GRB in terms of the duration reported in the GBM GRB catalog (von Kienlin et al. 2020), with $T_{90}(50\text{–}300\,\mathrm{keV}) = 3.7 \pm 0.6$ s. For the GBM, von Kienlin et al. (2020) found that the threshold separating short and long GRBs is $T_{90} = 4.2$ s—instead of the $T_{90} \approx 2$ s of the Burst And Transient Source Experiment (BATSE; Kouveliotou et al. 1993).

3.4. Spectral Properties of the Prompt Gamma-Ray Emission

We performed a Swift BAT and Fermi GBM joint spectral fit in RMFit[18] v4.3.2. We used the GBM time-tagged events (TTE) data from the NaI 3/4 and BGO 0/1 detectors, from which we selected the 8−900 keV and 200 keV−40 MeV spectral regimes, respectively. The 15−150 keV BAT spectra were extracted with the *batbinevt* tool. Using C-statistics, we modeled the νF_ν spectrum of the ≈0.3 s short GRB with a simple power law. A power-law model overestimates the data over ≈1 MeV; consequently, we modeled the high-energy break with a cutoff power-law model (see, e.g., Poolakkil et al. 2021). The best-fitting model suggests that the νF_ν spectrum has a hard slope with mean photon index $\beta_{\mathrm{PI}} = -\alpha_{\mathrm{CL}} = 0.63 \pm 0.05$, peak energy $E_{\mathrm{peak}} = 2290 \pm 238$ keV, and fluence $S(10\text{–}10^4\,\mathrm{keV}) = (5.6 \pm 0.4) \times 10^{-6}$ erg cm^{-2}. The photon index is average compared to other short hard GRBs detected by the GBM (von Kienlin et al. 2020; Poolakkil et al. 2021). Yet, GRB 180618A is one of the hardest and most energetic gamma-ray pulses among short GRBs; it is within the ≈1% percentile in terms of the high-frequency peak energy and within the top ≈5% in terms of the total energy released (see Figures 9(b), (c)).

For the spectrum corresponding to the ≈0.3–45 s extended gamma-ray emission, the best-fitting photon index of the power-law model is $\beta_{\mathrm{PI}} = 1.51 \pm 0.09$. This intermediate photon index suggests that the spectrum has a cutoff (e.g., Poolakkil et al. 2021). In order to constrain the peak energy, we fixed the low-energy index of the cutoff power-law model to the average of the GBM catalog (Poolakkil et al. 2021) of short ($\alpha_{\mathrm{CL}} = -0.6$) and long GRBs ($\alpha_{\mathrm{CL}} = -1$). We find $E_{\mathrm{peak}} = 87 \pm 18$ keV and $S(10\text{–}10^4\,\mathrm{keV}) = (6 \pm 1) \times 10^{-7}$ erg cm^{-2} for $\alpha_{\mathrm{CL}} = -0.6$, and $E_{\mathrm{peak}} = 125 \pm 45$ keV and $S(10\text{–}10^4\,\mathrm{keV}) = (8 \pm 2) \times 10^{-7}$ erg cm^{-2} for $\alpha_{\mathrm{CL}} = -1$, consistent with the Svinkin et al. (2018) findings.

To determine the temporal evolution of the photon index and the peak energy, we fitted a cutoff power-law model to the 8 keV−40 MeV GBM spectrum of each light-curve bin. To avoid merging peaks and valleys, we used a constant binning as opposed to a fixed signal-to-noise ratio (e.g., Guiriec et al. 2010). Using the default 64 ms binned light curves, we find that in a time span of less than 260 ms, the peak energy increases from $E_{\mathrm{peak}} = 427 \pm 138$ keV to $E_{\mathrm{peak}} = 2593 \pm 473$ keV with constant photon index. As seen in other spectroscopically resolved short GRBs (Guiriec et al. 2010), the peak energy tracks the light curve with a strong soft–hard–soft spectral evolution in a short time period; see the peak energy evolution in Figure 1(b) and the photon index in Figure 2 (bottom panel).

3.5. Intrinsic Energetics

Short GRBs have typically lower fluences and thus follow a different peak energy (E_{peak}) and isotropic energy (E_{iso}) relation than long GRBs (Amati 2006; Ghirlanda et al. 2009). If we introduce the k-correction (Bloom et al. 2001) to the $1-10^4$ keV rest-frame energy band for redshift $z = 0.554$, we obtain an isotropic-equivalent energy $E_{\mathrm{iso}} = (4.6 \pm 0.4) \times 10^{51}$ erg and luminosity $L_{\mathrm{iso}} = (1.9 \pm 0.2) \times 10^{52}$ erg s^{-1} for short GRB 180618A, and $E_{\mathrm{iso}} = (7 \pm 2) \times 10^{50}$ erg and $L_{\mathrm{iso}} = (2.4 \pm 0.7) \times 10^{49}$ erg s^{-1} for the extended gamma-ray emission. See also the high-energy properties for redshifts $z = 0.01$–1.5 in Figure 10. For redshifts $z \gtrsim 0.1$, GRB 180618A lays within the cluster of short GRBs—it is one of the hardest

[18] https://fermi.gsfc.nasa.gov/ssc/data/analysis/rmfit/